Zeros in the photoionization partial cross sections of H_2^+

R. Della Picca, P. D. Fainstein,* and M. L. Martiarena
Centro Atómico Bariloche, Comisión Nacional de Energía Atómica, Avda E. Bustillo 9500, 8400 Bariloche, Argentina

A. Dubois
Laboratoire de Chimie Physique-Matière et Rayonnement, Université Pierre et Marie Curie, 11 rue Pierre et Marie Curie, 75231 Paris Cedex 05, France

(Received 25 November 2007; published 5 February 2008)

The partial cross sections for photoionization of H_2^+ present structures which are usually called Cooper-like minima. We analyze the physical origin of these features to determine if they are associated to the confinement of the target electron, as recently proposed by Férnandez *et al.*, or to zero absorption as suggested here. A thorough analysis of the partial cross sections, the phase shifts, and the transition amplitude clearly shows that the Cooper-like minima correspond to zero absorption. To demonstrate this we show that the phase shifts have a maximum and the transition matrix is exactly zero at the electron momentum corresponding to where the Cooper-like minima appear. Finally, we show that the existence of the Cooper-like minima survive when the vibrational degree of freedom of the target is taken into account.

DOI: 10.1103/PhysRevA.77.022702 PACS number(s): 33.80.Eh

I. INTRODUCTION

Very recently there has been a renewed interest in the study of angular distributions in photoionization of H_2^+ [1–4]. This system provides an ideal benchmark to test theoretical models to treat molecular photoionization. Particularly, it allows us to compare results from exact calculations [1–4] with theoretical models which employ perturbative approximations to the bound and continuum states [5,6]. The same model system has also attracted the attention for the study of photoionization by high-intensity ultrashort laser pulses [7].

In a recent paper [8] the photoionization of H_2 and H_2^+ molecules was investigated for photon wavelength such that the de Broglie wavelength of the ejected electron is comparable or smaller to the internuclear distance. For such case of fast photoelectrons the angular distribution shows some very interesting and unexpected features. Surprisingly, since the electrons move rapidly away from the target, the angular distribution shows a strong dependence on the vibrational state of the residual target. Also, the integrated cross sections as a function of photon energy for different partial waves show distinct minima which occur approximately when the relation $k_eR=l\pi$ between the photoelectron momentum k_e, the internuclear distance R, and the partial wave l is verified. It was found, however, that this only occurs for parallel alignment of the molecular axis with respect to the polarization vector. As this formula describes momentum quantization in a box of length R, the authors of Ref. [8] suggested that the minima in the spectra can be related to electron confinement at the given value of R. As a proof of this proposal it was verified that the nodal structure of the continuum wave function at the corresponding k_e value reproduces that of the initial state inside the internuclear region.

The existence of minima in the partial cross sections has been reported already for photoionization of H_2^+ [2], H_2 [9], and N_2 [10,11]. It is a phenomena independent of the initial and final vibrational state of the molecule and is usually referred to as "Seaton-Cooper minima" for atomic targets and "Cooper-like minima" for molecular targets, following their discovery by Seaton [12] and Cooper [13] in the photoionization spectra of atoms [14]. In all these previous works, Cooper-like minima were found for fixed values of the internuclear distance corresponding to the equilibrium distance of the molecules.

To analyze in more detail these features we present here a thorough investigation of the partial cross sections in a wide range of internuclear distances and electron momenta. For simplicity we consider the case of a one-electron molecule since this problem can be solved exactly and contains all the physics. We consider the partial wave contribution to the integrated cross section for parallel alignment of the molecular axis with respect to the linear polarization of the photon field. Atomic units will be used except when otherwise stated.

II. THEORY

We consider the photoionization of a one-electron diatomic molecule. The nuclei of the molecule have charge Z_a and Z_b and are fixed at the internuclear distance R. Using standard methods we calculate exactly the initial ground [15] and final continuum [16,17] states of the molecule. Within the dipole approximation we calculate the partial cross sections [18] which are given by

$$\sigma_{lm} = \frac{4\pi^2\alpha\omega}{3}|M_{lm}|^2, \tag{1}$$

where α is the fine structure constant, $\hbar\omega$ is the photon energy, and the transition amplitude is given by

$$M_{lm} = \langle \psi_{mq}^{(-)}(\mathbf{k}_e,\mathbf{r})|\hat{\varepsilon}\cdot\mathbf{D}|\psi_i(\mathbf{r})\rangle \tag{2}$$

with $\mathbf{k}_e \equiv \{k_e,\theta_e,\phi_e\}$ the ejected electron momentum in the molecular frame and $E_e=k_e^2/2$ the corresponding photoelec-

*pablof@cab.cnea.gov.ar

tron energy. The dipole operator $\mathbf{D}$ in Eq. (2) is given by $\mathbf{D}=\boldsymbol{\nabla}/\omega$ or $\mathbf{D}=\mathbf{r}$ in the velocity and length gauges, respectively. We calculate the partial cross sections in both gauges to check the numerical accuracy of the different integration schemes and find in all cases perfect agreement. The partial wave $\psi_{mq}^{(-)}$ describes an electron with momentum $\mathbf{k}_e$ moving in the two-center continuum and can be represented in spheroidal coordinates (ξ,η,φ) as the product [19]:

$$\psi_{mq}^{(-)}(\mathbf{k}_e,\mathbf{r}) = (2\pi)^{-1/2} e^{\pm im\varphi} \Pi_{mq}(c,a;\xi)\Xi_{mq}(c,b;\eta), \quad (3)$$

where $m=0,1,2,\ldots$ is the magnetic quantum number, $q=0,1,2,\ldots$ is the number of zeros of the quasiangular spheroidal function $\Xi_{mq}(c,b;\eta)$ in the interval $\eta\in(-1,1)$, $l=q+m$, $c=k_eR/2$, $a=R(Z_a+Z_b)$, and $b=R(Z_a-Z_b)$. The quasiradial spheroidal function $\Pi_{mq}(c,a;\xi)$ has the appropriate asymptotic conditions:

$$\Pi_{mq}(c,a;\xi) = (c\xi)^{-1} N_{mq}(c,a,b)\sin \times\left(c\xi + \frac{a}{2c}\ln 2c\xi - \frac{\pi l}{2} + \Delta_{mq}\right) + O[(c\xi)^{-2}] \quad (4)$$

with $\xi\in(1,+\infty)$. $\Delta_{mq}=\Delta_{mq}(k_e,R)$ is the phase shift of the two-center problem and $N_{mq}=(2k_e/\pi)^{1/2}$ is the normalization coefficient. The phase shift is normalized using the condition $\Delta_{mq}(k_e,0)=\sigma_l(k_e)$, where $\sigma_l(k_e)$ is the phase shift corresponding to a Coulomb potential with nuclear charge $Z=Z_a+Z_b$ and angular momentum l. We can thus define

$$\Delta_{mq}(k_e,R) = \Delta_{mq}(k_e,0) + \delta_{mq}(k_e,R), \quad (5)$$

where $\Delta_{mq}(k_e,0)$ is the asymptotic Coulomb phase shift and $\delta_{mq}(k_e,R)$ is the additional phase shift which provides all the information about the interaction with the two-center potential. The properly normalized $1s\sigma_g$ initial ground state $\psi_i(\mathbf{r})$ can also be written in spheroidal coordinates as [15]

$$\psi_i(\mathbf{r}) = (2\pi)^{-1/2}\Lambda(\xi)M(\eta). \quad (6)$$

Performing the integration over the azimuthal angle φ, the transition matrix (2) can be cast into the form

$$M_{lm} = \frac{(\hat{\varepsilon}\cdot\hat{z})}{\omega}\delta_{m0}\mathcal{M}_{l0} + \left[\frac{(\hat{\varepsilon}\cdot\hat{x}) - i(\hat{\varepsilon}\cdot\hat{y})}{2\omega}\delta_{m1} + \frac{(\hat{\varepsilon}\cdot\hat{x}) + i(\hat{\varepsilon}\cdot\hat{y})}{2\omega}\delta_{m-1}\right]\mathcal{M}_{l1}, \quad (7)$$

where $\mathcal{M}_{lm}$ are reduced matrix elements which only involve the integration over the quasiangular (η) and quasiradial coordinates (ξ). The coordinates $(\hat{x},\hat{y},\hat{z})$ represent a reference frame fixed on the molecular center of mass with the $\hat{z}$ direction oriented along the internuclear axis (see Fig. 1 in Ref. [2]).

Due to the symmetries of the initial ground state and the dipolar operator, the projection of the angular momentum operator m can only take the values 0 $(\sigma\to\sigma)$ and 1 $(\sigma\to\pi)$. Moreover, for parallel alignment between the internuclear distance and the polarization vector only $\sigma\to\sigma$ transitions can occur, while for the perpendicular arrangement only $\sigma\to\pi$ transitions are allowed. The partial cross sections for these transitions are determined by the reduced matrix elements $\mathcal{M}_{l0}$ and $\mathcal{M}_{l1}$, respectively [see Eq. (7)]. For homonuclear molecules, like H_2^+, the angular momentum quantum number l can only take odd values.

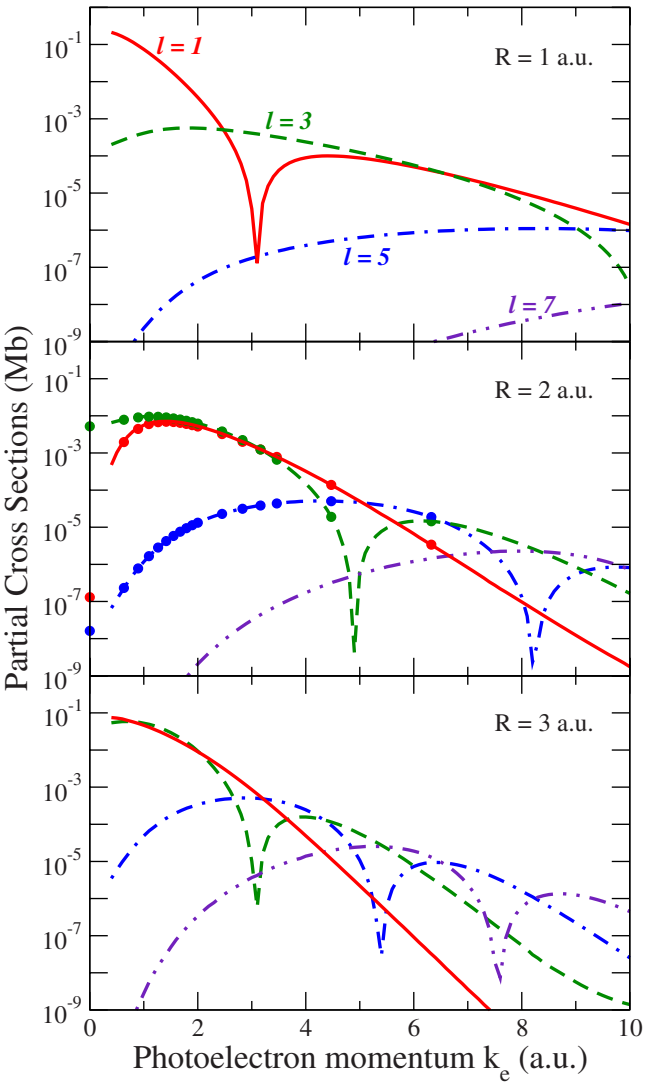

FIG. 1. (Color online) Partial cross section σ_{l0} as a function of photoelectron momentum k_e for internuclear distance $R=1$, 2, and 3 a.u. Solid line, $l=1$; dashed line, $l=3$; dot-dashed line, $l=5$; double-dot dashed line, $l=7$; (●), from Ref. [18].

III. RESULTS AND DISCUSSION

A. Cooper-like minima in the partial cross sections

We calculate the partial cross sections for parallel alignment between the internuclear axis and the polarization vector (σ_{l0}), for different values $l=1$, 3, 5, and 7 in a wide range of k_e and R values. In Fig. 1 we present σ_{l0} for $l=1,3,5,7$ as a function of k_e for $R=1,2,3$ a.u. For $R=2$ a.u. we include in the figure the results from Ref. [18] which coincide exactly with our results. From the figure it results that all the partial cross sections present Cooper-like minima. For a fixed value of R the minima appear at higher values of k_e as l increases, in agreement with the empirical formula k_eR

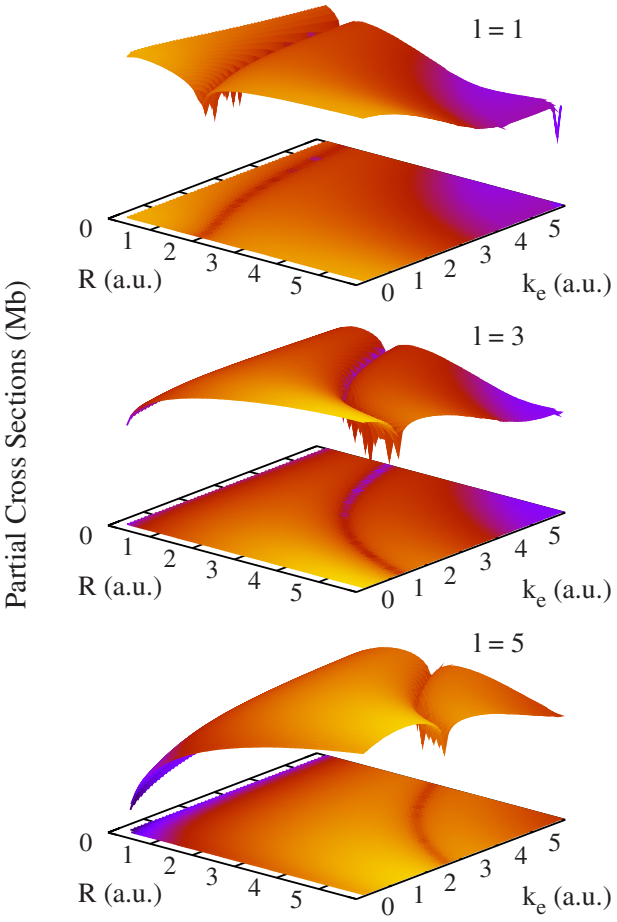

FIG. 2. (Color online) Partial cross section σ_{l0} as a function of the photoelectron momentum k_e and the internuclear distance R, for $l=1,3,5$.

$=l\pi$ of Ref. [8]. Also, for a fixed value of l the Cooper-like minima shift to lower values of k_e as R increases. Let us consider, in particular, the $l=1$ minima. It can be found at $k_e \simeq 3$ a.u. for $R=1$ a.u. When R increases up to 2 a.u. it seems to be at the threshold energy and then it disappears for higher internuclear distances. This result explains the nondipolar behavior of the angular distribution at low energies for molecules like H_2^+ and N_2, which have an equilibrium internuclear distance close to 2 a.u. [3]. It is interesting that for $R=3$ a.u. this partial cross section rises close to threshold instead of falling. Following the arguments of Connerade (see p. 115 in Ref. [14]), the reason could be that due to the continuity between excitation and ionization the Cooper-like minima move below threshold and would thus appear as a minimum in the photoabsorption cross section.

In Fig. 2 we summarize all the results of the present calculation plotting in three dimensions the partial cross sections for $l=1,3,5$ as a function of k_e and R in a much extended range. We vary R from 0.3 up to 6 a.u. with step $\Delta R=0.1$ a.u. The minima now form a considerable structure that varies continuously and seems to follow the relation $k_eR=l\pi$. To verify this quantitatively we plot in Fig. 3 the position of the minima in the k_eR plane and compare with the relation $k_eR=l\pi$. We use a logarithmic scale to better visualize the similarities and discrepancies. For each partial wave

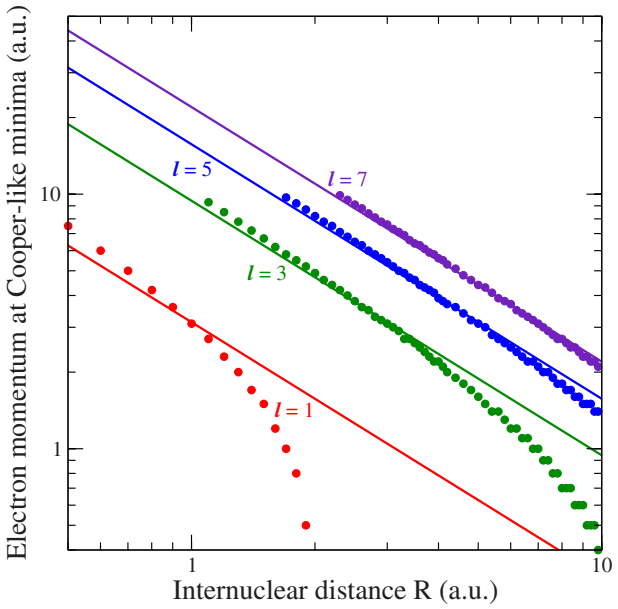

FIG. 3. (Color online) Photoelectron momentum corresponding to the Cooper-like minima as a function of the internuclear distance R, for $l=1,3,5,7$.

we note a good agreement at high values of k_e and large discrepancies as k_e becomes smaller than a few atomic units. For $l=1$ we notice that as R increases the curve tends to saturate at $R \simeq 2$ a.u. This means that for larger values of R the p-partial cross section has no Cooper-like minima and it is thus a monotonic decreasing function of k_e [see, for example, Fig. 1(c)]. As discussed in the previous paragraph this means that the Cooper-like minima has moved below threshold. In fact, the same happens with the higher partial waves, as can be seen in the figure for $l=3$, but for much larger values of R.

We conclude therefore that the Cooper-like minima are a general feature of all partial waves. As proposed in Ref. [8] their positions in the spectra follow approximately the relation $k_eR=l\pi$ which we show to be valid only for high enough photoelectron energy.

B. Electron confinement

In their paper, Fernández *et al.* [8] introduced the notion of electron confinement associated to the minima in the partial cross sections for polarization parallel to the internuclear vector. In that case the authors discuss the fact that electron emission does not follow the direction of polarization since it is suppressed by the confinement of the electrons along the internuclear distance.

In the previous section we have shown that the suppression of electron emission can also be attributed to the appearance of Cooper-like minima. For atomic targets, it is well known that the Seaton-Cooper minima arise when the transition matrix vanishes exactly corresponding therefore to zero absorption at the particular photon energy [14]. The ideas of confinement and no absorption are indeed mutually exclusive since the first simply addresses a tendency, a propensity, while the second is a strict criterion. We therefore

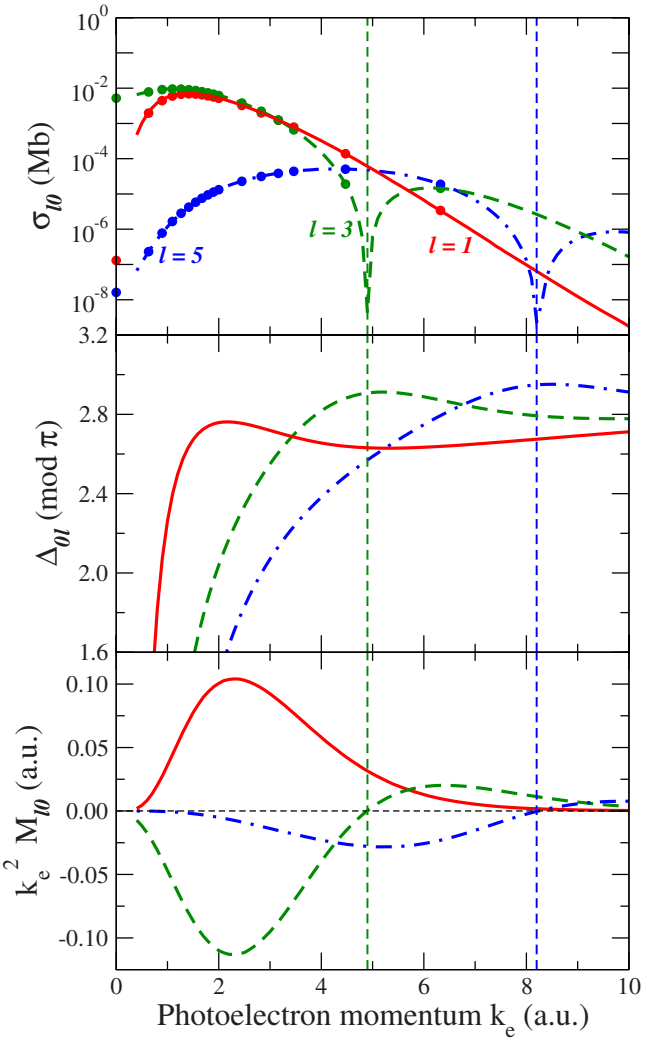

FIG. 4. (Color online) Partial cross section σ_{l0}, phase shift $\Delta_{0l}(k_e,R)$, and transition matrix M_{l0} [see Eqs. (1), (5), and (2)] as a function of photoelectron momentum k_e for $R=2$ a.u. Solid line, $l=1$; dashed line, $l=3$; dot-dashed line, $l=5$; (●), from Ref. [18]. The transition matrix has been multiplied by k_e^2 to enhance the values at large k_e and thus improve the visibility of the effect.

propose to find out which one really explains the data for molecular targets. For atomic targets the Seaton-Cooper minima appear for $l \rightarrow l+1$ transitions provided that the radial wave function of the initial state has at least one node. Since the ground state of H_2^+ does not have a node, the Cooper-like minima were explained as being due to the nonspherical shape of the molecular potential [9].

The concept of zero absorption in photoionization can be related to that of no scattering in elastic collisions, as in the Ramsauer-Townsend effect [20]. In the latter, a given partial cross section (usually the *s* wave) shows a minima which is related to a rapid variation of the phase shift. We plot therefore in Fig. 4 the partial cross sections, the phase shifts, and the transition matrix given by Eqs. (1), (5), and (2), respectively, as a function of electron momentum. We consider the equilibrium internuclear distance ($R=2$ a.u.) and the $l=1,3,5$ partial waves. Interestingly, as can be seen from the figure, we find that for $l=3$ and 5 the Cooper-like minima are

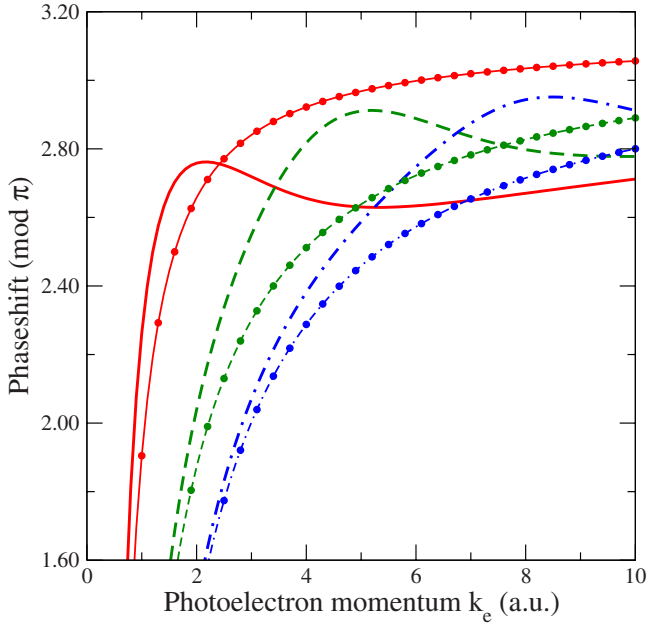

FIG. 5. (Color online) Coulomb $\Delta_{0l}(k_e,0)$ (lines with circles) and additional phase shift $\delta_{0l}(k_e,R)$, see Eq. (5), as a function of photoelectron momentum k_e for $R=2$ a.u. and $l=1$ (solid lines), $l=3$ (dashed lines), and $l=5$ (dot-dashed line).

associated to a maximum in the corresponding phase shifts and that the transition matrix is exactly zero at the particular value of electron momentum. To see the reason for this behavior we plot in Fig. 5 the Coulomb $\Delta_{mq}(k_e,0)$ and additional phase shifts $\delta_{mq}(k_e,R)$ for this case. The former is a smooth function of electron momentum while the latter presents a maximum, showing therefore that the molecular potential at short distances is responsible for the minima in the partial cross sections. However, the positions of these maxima do not coincide with the positions of the Cooper-like minima. The latter are determined by the positions of the maxima in the total phase shift $\Delta_{mq}(k_e,R)$. We conclude therefore that the Cooper-like minima for the molecular target are due to the molecular potential and to the corresponding phase shifts which present a maximum in the electron momentum range where the minimum appears. Following our hypothesis at the beginning of this paragraph this result implies therefore that the minima are clearly associated to zero absorption.

The following question that we wish to address is how the variation of the phase shifts translates into a zero value of the transition matrix. This is straightforward for elastic collisions, but not so in the present case where the phase shifts do not appear explicitly in the expression for the transition matrix. We analyze therefore in detail the wave functions and the transition matrix. Fernández *et al.* [8] noted that the electron continuum wave function reproduces the nodal structure of the initial bound state for the electron momentum values where the minima show up. In Fig. 6 we plot the initial bound and final continuum states for $R=2$ a.u., $l=3$, and $k_e=4,4.9,6$ a.u., which correspond to values smaller, equal, and larger to the k_e value where the minima appear. In Fig. 6, upper panel, we plot the wave functions as a function of the

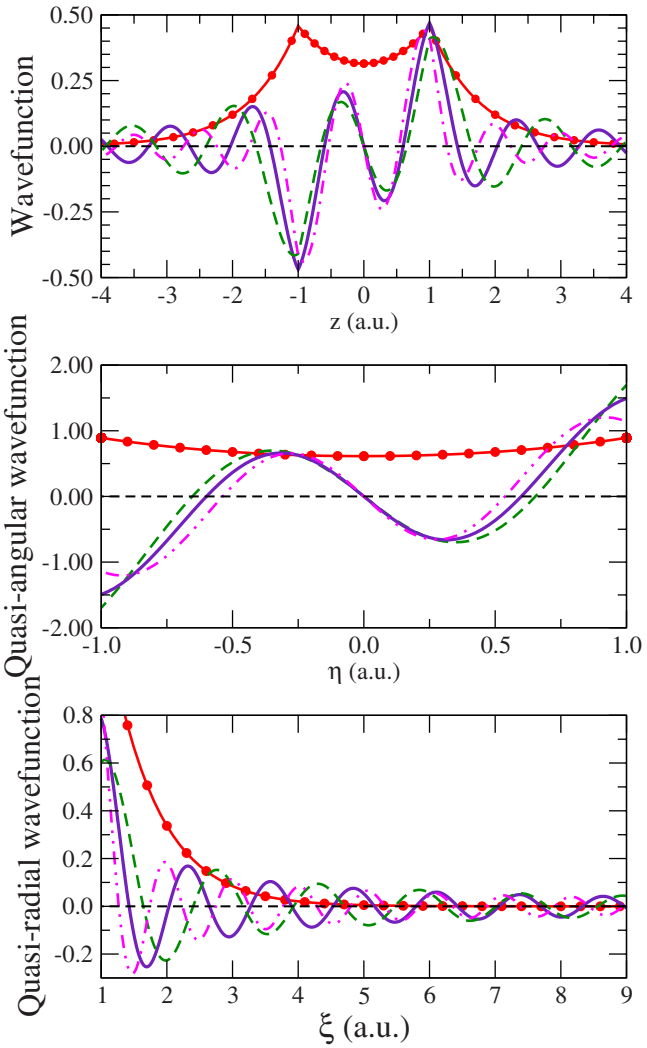

FIG. 6. (Color online) Initial bound (solid line with circles) and final continuum wave function, for k_e=4 (dashed line), 4.9 (solid line), and 6 (dot-dashed line) a.u., as a function of the internuclear z (upper panel), quasiangular η (middle panel), and quasiradial ξ (lower panel) coordinates.

coordinate in the internuclear direction (z). We can see that indeed only for k_e=4.9 a.u. the positions of the maxima of the initial state coincide exactly with the main maxima and minima of the final continuum state. The overlap between these states is thus zero. However, this does not imply that the transition matrix is zero since this plot just represents a cut of the wave functions in a particular plane. Strictly speaking, the overlap between the initial and all final continuum states should be zero as they are orthogonal. The transition matrix involves the dipole operator and thus the problem is far more complicated. In fact, from this figure one could naively conclude that since the initial state is even, the final continuum state odd, and the dipole operator odd, the transition amplitude is never zero. Of course this is because this plot just represents a part of the wave functions. In our present calculations we employ spheroidal coordinates which are particularly well suited for the two-center potential. In Fig. 6 we also plot the quasiangular (middle panel) and quasiradial (lower panel) initial and final wave functions. In this case, the plots correspond to the full wave functions and not to a given cut. In the latter we can observe how as the electron momentum increases the continuum wave functions penetrate more into the potential. Again, from these figures we cannot determine why the transition matrix is zero just for k_e=4.9 a.u. To answer this we have to analyze in detail the transition matrix.

As noted in Sec. II the partial cross sections are determined by the reduced matrix elements. Since we are here concerned with $\sigma \rightarrow \sigma$ transitions we analyze in detail $\mathcal{M}_{l0}$ which in the velocity gauge and after some algebra is given by

$$\mathcal{M}_{l0} = \left(\frac{R}{2}\right)^2 [A^l_\xi(k_e,R)B^l_\eta(k_e,R) + B^l_\xi(k_e,R)A^l_\eta(k_e,R)], \quad (8)$$

where

$$A^l_\xi(k_e,R) = \int_1^\infty d\xi(\xi^2-1)\Pi_{0l}(c,a;\xi)\frac{\partial\Lambda(\xi)}{\partial\xi},$$

$$B^l_\xi(k_e,R) = \int_1^\infty d\xi\ \xi\Pi_{0l}(c,a;\xi)\Lambda(\xi),$$

$$A^l_\eta(k_e,R) = \int_{-1}^1 d\eta(1-\eta^2)\Xi_{0l}(c,b;\eta)\frac{\partial M(\eta)}{\partial\eta},$$

$$B^l_\eta(k_e,R) = \int_{-1}^1 d\eta\ \eta\Xi_{0l}(c,b;\eta)M(\eta).$$

These factors are obtained numerically, and plotted independently in Fig. 7 as a function of the electron momentum, for R=2 a.u. and l=3. The integrals B^l_ξ and B^l_η are never zero, as can be expected from the form of the quasiangular and quasiradial wave functions shown in Fig. 6. On the contrary, the integrals A^l_ξ and A^l_η are both zero for values of k_e close but not equal to that corresponding to the Cooper-like minimum. It is therefore the subtle combination of the four integrals in Eq. (8) which cancels and makes zero the transition matrix leading to a zero in the partial cross section. It is interesting to note that in the atomic case, as the initial state has a node, the integrals split into two contributions of opposite sign. The balance between this contribution cancels for a particular value of the electron momentum corresponding to the Seaton-Cooper minima (see p. 115 of Ref. [14]).

IV. VIBRATIONAL MOTION

The Cooper-like minima are structures which arise from the properties of the electronic transition matrix. In experiments it is, however, not possible to isolate the electronic from the vibrational motion. As is well known the differential and total cross sections will depend on the vibrational states of the target before and after the electron is emitted [11,21]. While our study is mainly devoted to analyze the origin of the Cooper-like minima it is also interesting to see how these structures would appear in experiments. This kind of study has already been performed for H_2 [8,9] and N_2

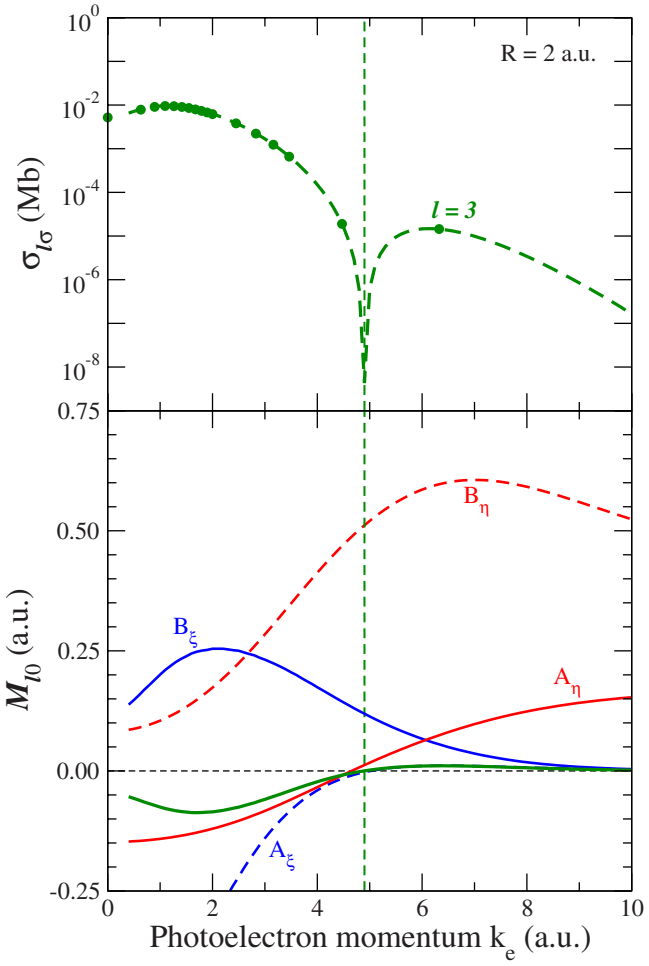

FIG. 7. (Color online) Partial cross section σ_{l0} and reduced matrix element $\mathcal{M}_{l0}$, see Eq. (7), as a function of photoelectron momentum k_e for $R=2$ a.u. and $l=3$. All quantities are defined in Eq. (8).

[11], to cite just a few examples. Following the work of Liu *et al.* [11] we calculate the vibrational unresolved partial cross section as

$$\sigma_{lm} = \frac{4\pi^2\alpha\omega}{3}\sum_{\nu'} |M_{lm}^{\nu\nu'}|^2, \tag{9}$$

where the transition matrix is given by

$$M_{lm}^{\nu\nu'} = \int dR \chi_{\nu'}^{(f)}(R) M_{lm}(R) \chi_{\nu}^{(i)}(R) \tag{10}$$

with $\chi_\nu^{(i)}$ ($\chi_{\nu'}^{(f)}$) the initial (final) vibrational state wave functions and M_{lm} the electronic transition matrix given by Eq. (2) which is a function of the internuclear distance R. This calculation is of course valid within the Born-Oppenheimer approximation which is assumed in the present work. We assume that in the initial state only the vibrational ground state ($\nu=0$) is populated and consider final vibrational states with $\nu'=0,1,2,3$. The results of this calculation is presented in Fig. 8 where we show the partial cross sections for different values of l both with and without taking into account the

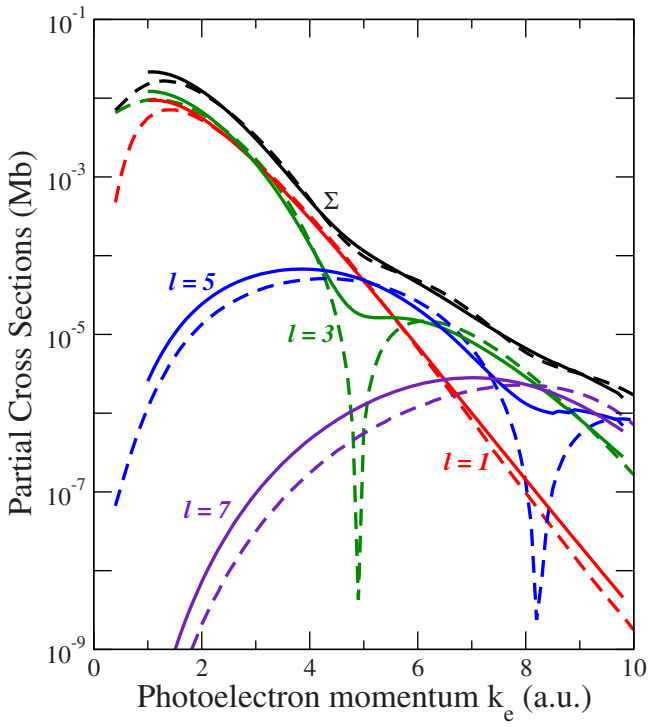

FIG. 8. (Color online) Dashed line: partial σ_{l0} and total cross section (indicated by Σ) as a function of photoelectron momentum k_e for internuclear distance $R=2$ a.u. Solid line: partial and σ-total cross section including vibrational transitions.

vibrational motion. In the latter case we consider that the molecule is at the equilibrium internuclear distance $R=2$ a.u. As in previous studies for H_2 [9] we find that when the vibrational motion is included, the sharp Cooper-like minima for $l=3$ and 5, which correspond to a zero in the partial cross section as shown in the present work, appear as wide minima in the partial cross section. When all the partial cross sections are summed the result is that the σ-total cross section (indicated by Σ in the figure) shows two humps and nonmonotonic decreasing behavior. In summary we find that, as was recently shown for N_2 [11], the Cooper-like minima produce observable effects even in the total cross section.

V. CONCLUSIONS

In summary, we have shown that the minima in the partial cross sections are Cooper-like minima which correspond to zero absorption. The position of these minima are given by the relation $k_eR=l\pi$ only at high enough values of k_e. Large discrepancies appear for k_e values smaller than a few atomic units for the p- and f-partial cross section, which give the main contribution to the total cross section in this energy range.

A detailed study of the Cooper-like minima shows that this large variation of the partial cross section occurs when the corresponding phase shift goes through a maximum. At this value of the electron momentum the transition amplitude is exactly zero and thus there is no absorption. This effect produces also a visible effect in the total cross section.

[1] T. N. Rescigno, D. A. Horner, F. L. Yip, and C. W. McCurdy, Phys. Rev. A **72**, 052709 (2005).
[2] R. Della Picca, P. D. Fainstein, M. L. Martiarena, and A. Dubois, J. Phys. B: At. Mol. Opt. Phys. **39**, 473 (2006).
[3] R. Della Picca, P. D. Fainstein, M. L. Martiarena, and A. Dubois, Phys. Rev. A **75**, 032710 (2007).
[4] M. Foster, J. Colgan, O. Al-Hagan, J. L. Peacher, D. H. Madison, and M. S. Pindzola, Phys. Rev. A **75**, 062707 (2007).
[5] M. Walter and J. Briggs, J. Phys. B: At. Mol. Opt. Phys. **32**, 2487 (1999).
[6] G. L. Yudin, S. Chelkowski, and A. D. Bandrauk, J. Phys. B: At. Mol. Opt. Phys. **39**, L17 (2006).
[7] S. Selstø, J. F. McCann, M. Førre, J. P. Hansen, and L. B. Madsen, Phys. Rev. A **73**, 033407 (2006).
[8] J. Fernández, O. Fojón, A. Palacios, and F. Martín, Phys. Rev. Lett. **98**, 043005 (2007).
[9] S. K. Semenov and N. A. Cherepkov, J. Phys. B **36**, 1409 (2003).
[10] S. K. Semenov, N. A. Cherepkov, M. Matsumoto, T. Hatamoto, X.-J. Liu, G. Prümper, T. Tanaka, M. Hoashino, H. Tanaka, F. Gel'mukhanov, and K. Ueda, J. Phys. B: At. Mol. Opt. Phys. **39**, L261 (2006).
[11] X.-J. Liu, N. A. Cherepkov, S. K. Semenov, V. Kimberg, F. Gel'mukhanov, G. Prümper, T. Lischke, T. Tanaka, M. Hoshino, H. Tanaka, and K. Ueda, J. Phys. B: At. Mol. Opt. Phys. **39**, 4801 (2006).
[12] M. J. Seaton, Proc. R. Soc. London, Ser. A **208**, 408 (1951); **208**, 418 (1951).
[13] J. W. Cooper, Phys. Rev. **128**, 681 (1962).
[14] J. P. Connerade, *Highly Excited Atoms* (Cambridge University Press, Cambridge, England, 1998).
[15] G. Hadinger, M. Aubert-Frécon, and G. Hadinger, J. Phys. B **22**, 697 (1989).
[16] L. I. Ponomarev and L. N. Somov, J. Comput. Phys. **20**, 183 (1976).
[17] J. Rankin and W. R. Thorson, J. Comput. Phys. **32**, 437 (1979).
[18] J. A. Richards and F. P. Larkins, J. Phys. B **19**, 1945 (1986).
[19] D. I. Abramov, A. Ya Kazakov, L. I. Ponomarev, S. Yu Slavyanov, and L. N. Somov, J. Phys. B **12**, 1761 (1979).
[20] C. J. Joachain, *Quantum Collision Theory* (North-Holland, Amsterdam, 1983).
[21] F. Martín, J. Phys. B: At. Mol. Opt. Phys. **32**, 501 (1999).